SHIHAB JOURNAL OF HUMANITIES
Volume (2), Issue (4) (October, 2026)
ISSN: 3136-2958

مجلة الشهاب للعلوم الإنسانية
المجلد (2) العدد(4) اكتوبر 2026
عدد خاص بالمؤتمر الدولي الأول لسلاسل الامداد والتوريد والإدارة اللوجستية في ليبيا
26-27 أغسطس 2026

An Integrated Risk Assessment Framework for Coastal Road Deterioration and Supply Chain Resilience

Mohammad Abdel Nasser Al-Warfalli, Material Engineer Academy for Postgraduate Studies, Libya, Mohammedalwera@gmail.com [1]
Muhammed S. Maddi , Researcher, Libyan Authority For Scientific, Libya, Muhammed.maddi2@gmail.com [2]

Received: 29/6/2026 Revised: 05/7/2026 Accepted: 28/7/2026 Publication: 5/10/2026

ABSTRACT:
Problem: Roads are a crucial component of any country's infrastructure and play a vital role in its sustainable economic development. Road quality is a key indicator of quality of life and economic competitiveness. Therefore, it is essential for governmental and economic entities, such as ministries and municipalities, to maintain road networks at appropriate quality levels and adhere to safety standards. This research aims to investigate the deterioration of coastal roads in hot cities, which is experiencing accelerated decline due to the complex interaction of factors that cause road collapse. These factors include high temperatures (reaching up to 47°C), high relative humidity (62-67%), and heavy traffic (more than 600,000 vehicles daily by 2026). This is particularly relevant given the lack of assessment models that integrate these factors with their direct impact on supply chains. This led to the development of the CRAAM model, which studies the six factors of deterioration: crack propagation, moisture damage, thermal stress, permanent deformation, cumulative wear, and asphalt performance. The polymer-modified deterioration index (DI) was weighted using hierarchical analysis with a CR consistency ratio of 0.07. Probability was also added using
Monte Carlo simulation (10,000 iterations) to account for uncertainties in the DI. Three studies from Tripoli showed that the combined effect accelerates deterioration and failure by 50%, and that delays in maintenance and early detection increase road lifecycle costs by more than 60-63%, and the likelihood of supply chain delays and disruptions rises to 72% in critical sections.
Keywords: Pavement Deterioration , Coastal Roads CRAAM ,Supply Chain Management Predictive, Maintenance Planning , six factors of deterioration

1.1 Background and Problem Statement

Road networks form the backbone of national infrastructure, directly impacting economic productivity, the provision of public services, and the movement of citizens. In Libya, coastal roads, particularly in hot coastal cities like Tripoli, bear disproportionate loads of goods and passengers, making their maintenance a matter of national strategic importance. However, these roads operate under conditions that consistently exceed conventional design assumptions: ambient temperatures reaching 47°C, relative humidity between 62% and 67%, intense ultraviolet radiation, and a high traffic volume exceeding 600,000 vehicles per day (projected by the end of 2026). Field observations conducted in Tripoli between 2022 and 2024 recorded rutting depths of 20–35 mm on heavily trafficked roads, with crack severity rated as high in over 60% of the sections examined.

Despite these harsh operating conditions, maintenance practices in Libyan municipalities remain largely reactive. This traditional approach has serious consequences: a non-linear

increase in repair costs as pavements age; traffic disruptions and bottlenecks in material logistics; and missed opportunities for systematic and cost-effective planning. A major limitation lies in the analytical separation of deterioration mechanisms within current single-mechanism models, such as HDM-4 and PCI. These frameworks systematically underestimate actual deterioration rates by more than 30% compared to field measurements because they fail to account for the synergistic interactions between thermal, mechanical, and hydrological processes and material degradation processes. Furthermore, neither HDM-4 nor PCI integrates supply chain management as a variable in maintenance decision-making, a critical deficiency in logistically sensitive coastal environments.

1.2 Research Objectives

This study addresses identified shortcomings through the following objectives:

1. To develop an advanced mathematical framework for the simultaneous analysis of six interacting mechanisms of pavement deterioration in warm coastal environments.
2. To develop an advanced mathematical framework for the simultaneous analysis of six interacting mechanisms of pavement deterioration in warm coastal environments. To generate a standardized damage index (DI, from 0 to 10) using the Analysis Hierarchy Process (AHP) with the integration of uncertainty measurement using Monte Carlo simulation, enabling risk classification and maintenance prioritization.
3. To derive three formal equations that quantify the impact of the supply chain and correlate the damage index (DI) with increased logistics costs, the likelihood of delivery delays, and loss of transport efficiency.
4. To validate the framework using three documented failure cases in Tripoli and compare its predictive accuracy with HDM-4 and PCI standards.

1.3 Contribution to Research and Innovation

The CRAAM framework offers three innovative scientific contributions:

- First, it represents the first operational model to integrate the six major degradation mechanisms of hot coastal pavements into a single, mathematically consistent, PAJ-weighted index, thus surpassing the single-mechanism architecture of conventional systems such as HDM-4 (Table 2.1).
- Second, this model adds a probability layer of risk through Monte Carlo simulation, providing confidence intervals for the damage index that conventional deterministic models cannot generate.
- Third, this model formally links the structural state mechanisms of the pavement to supply chain performance through three calibrated impact equations, representing a new contribution to studies of pavement engineering in hot coastal areas.

II. LITERATURE REVIEW

2.1 Pavement Deterioration in Hot Environments :

Flexible pavement systems distribute traffic loads across sublayers to protect the underlying subgrade. In coastal and hot climates, environmental factors significantly accelerate structural degradation, reducing service life below design expectations. Al-Khateeb et al. (2021) and Zhang et al. (2023) demonstrated that single-mechanism models reduce field deterioration estimates by approximately 30%—a finding corroborated by monitoring data collected in Tripoli between 2022 and 2024. This systematic underestimation arises because sequential models process thermal, moisture, and mechanical effects independently, thereby neglecting the amplification that occurs when multiple mechanisms act concurrently.

2.2 Crack Propagation and Moisture Damage :

Cracking—longitudinal, transverse, and alligator patterns—represents one of the earliest and most diagnostic indicators of pavement distress. Field studies by Birgisson et al. (2010) and

Luo et al. (2021) documented that alligator cracking (fatigue cracking) induced by repeated traffic loads reduces structural capacity by 40% prior to intervention. Moisture damage occurs when water molecules displace asphalt binder from aggregate surfaces, reducing tensile strength and interparticle bonding. The Tensile Strength Ratio (TSR) quantifies moisture susceptibility; Values below 0.80 indicate unacceptable performance according to AASHTO T 283 standards (Caro et al., 2018; Moraes et al., 2017).

2.3 Rutting, Thermal Stress, and Time-Dependent Fatigue

Rutting originates from permanent longitudinal depressions in wheel paths caused by viscous flow of the binder at elevated temperatures. Studies in hot climates report average rut depths of 15–35 mm on roads where surface temperatures regularly exceed 55°C—consistent with field data from Tripoli (Brown & Cross, 2022; Pronk & Cocurullo, 2020). Thermal cycling induces tensile and compressive stresses, causing low-temperature cracking and high-temperature deformation. Ultraviolet radiation accelerates photo-oxidative hardening of the binder, leading to surface embrittlement (Dong & Huang, 2021). Time-dependent fatigue accumulates micro-damage under cyclic loading phenomenon without immediate failure, a captured by Miner's cumulative damage rule (Miner, 1945).

2.4 Polymer-Modified Binder (PMB)

Yusoff et al. (2011) and Cao et al. (2024) reported that polymer-modified asphalt containing 3–6% styrene-butadiene-styrene (SBS) by mass reduces rutting by 30–50%, improves stress resistance by 40–60%, and enhances moisture resistance relative to unmodified binders. However, while PMB improves surface layer properties, it does not compensate for structural deficiencies in underlying base or subgrade layers—a distinction of paramount importance for understanding the failure mechanism documented at Tripoli University Road (Section 4.2).

2.5 Supply Chain and Infrastructure Interdependence

Rodriguez (2023) and Rao and Chen (2022) documented that pavement deterioration increases vehicle operating costs, reduces average raising speeds, and causes delivery delays, transport costs by 20–45% on poorly maintained corridors. This disparity induces axle load redistribution, alternative route formation, and increased pavement roughness. Despite this well-established interdependence, conventional pavement frameworks do not routinely integrate supply chain impact into maintenance prioritization—the critical gap that CRAAM was designed to address.

2.6 Comparative Analysis of Existing Models

Previous studies address numerous factors influencing pavement deterioration; However, most adopt conventional, single-perspective approaches that either isolate deterioration mechanisms or treat road–supply chain relationships generically. Table 2.1 summarizes the comparative capabilities of CRAAM against HDM-4 and PCI.

Table 2.1
Capability Comparison: CRAAM, HDM-4, and PCI

Capability	HDM-4	PCI	CRAAM (This Study)
Multi-mechanism integration	Partial (sequential)	No	Yes 6 (simultaneous, 6 mechanisms)
AHP-weighted damage index	No	No	Yes (CR = 0.07)
Probabilistic uncertainty (Monte Carlo)	No	No	Yes (10,000 iterations)
Supply chain impact quantification	No	No	Yes (3 formal equations)
Hot coastal environment calibration	Limited	No	Yes (Tripoli 2022–2026)
Predictive maintenance scheduling	Partial	No	Yes (risk-tiered matrix)

Note. HDM-4 = Highway Development and Management Model; PCI = Pavement Condition Index.
Source: Developed by the authors.

III. METHODS AND MATERIAL

3.1 Research Design

This study follows a four-phase integrated design: (a) archival data collection for the period 2022–2026; (b) formulation of six sub-models for deterioration and failure mechanisms; (c) aggregation via the Analytic Hierarchy Process (AHP) into a unified damage index with Monte Carlo uncertainty quantification; and (d) estimation and calibration of supply chain impact through empirical equations. All calculations and analyzes were implemented in Python 3.11.

3.2 Data Inputs

Environmental and traffic input parameters for Tripoli are summarized in Table 3.1.

Table 3.1
Environmental and Traffic Input Criteria, Tripoli 2022–2026

Parameter	2022–2023	2023–2024	2024–2025	2025–2026
Max Temperature (°C)	40–46	43–47	44–46	40–44
Min Temperature (°C)	7–12	7–10	8–10	9–11
Avg Relative Humidity (%)	62–64	64–65	63–65	63–67
Annual Rainfall (mm)	290–320	247–320	247–280	220–280
Daily Traffic Volume	>500,000	>530,000	>550,000	>600,000
Level of Service	LOS E	LOS F	LOS F	LOS F

Source: Developed by the authors from meteorological and traffic authority records.

3.3 Mathematical Model Formulation

Crack Propagation — Paris–Erdogan Law 3.3.1

The crack growth rate is determined by Paris' Law:

$$\frac{da}{dN} = C \cdot (\Delta K)^m \quad \dots (1)$$

Where a is the crack length (mm), N is the number of load cycles, ΔK is the stress intensity factor range (MPa · $m^{0.5}$), and C and m are empirically calibrated material constants.

Moisture Damage — Tensile Strength Ratio 3.3.2

The moisture susceptibility is defined by the ratio of wet to dry tensile strength :

$$\text{TSR} = \frac{S_{wet}}{S_{dry}} \quad \dots (2)$$

Note: A TSR threshold ≤ 0.80 *defines unacceptable moisture susceptibility according to AASHTO T 283.*

3.3.3 Thermal Stress

The thermal stress (σ_T) in the pavement layer is calculated as:

$$\sigma_T = E \cdot \alpha \cdot \Delta T \quad \dots (3)$$

Where E is the elastic modulus (MPa), α is the thermal expansion coefficient ($^{\circ}C^{-1}$), and ΔT is the temperature differential (˚C).

3.3.4 Permanent Deformation Prediction

The rut depth (RD) is predicted using the following empirical model:

$$\text{RD} = a \cdot N^b \cdot T^c \quad \dots (4)$$

Where N represents the number of load cycles, T is the pavement temperature (˚C), and a, b, c are material coefficients.

3.3.5 Polymer Modification Performance

The performance improvement due to polymer modification is expressed as:

$$\text{PI} = \frac{E_{polymer}}{E_{base}} \quad \dots(5)$$

3.3.6 Integrated Damage Index

The integrated damage index (DI) is calculated as the weighted sum of individual damage components:

$$\text{DI}_{\text{raw}} = \sum (w_i \cdot DI_i); \quad \text{DI} = \min(\text{DI}_{\text{raw}}, 10) \quad \dots(6)$$

Each sub-index (DIi) is calibrated to the range [0, 10]. The capping function constrains the composite index to the defined scale. Values of exceeding 10 indicate complete structural failure under compound mechanism interaction—a physically meaningful condition represented by the capped value .

3.4 AHP Weight Derivation

Weights (w1) through (w6) were determined using the Analytic Hierarchy Process (AHP; Saaty, 1980) based on pairwise comparisons conducted by five infrastructure engineering expert . The resulting comparison matrix yielded a consistency ratio CR=0.07 (threshold ≤0.10), confirming acceptable expert judgment reliability.

Table 3.2
AHP Pairwise Comparison Summary and Derived Weights

Mechanism	Symbol	AHP Priority Weight (w_i)	Rank
Crack Propagation	DI_crack	0.28	1
Moisture Damage	DI_moisture	0.24	2
Rutting	DI_rutting	0.18	3
Thermal Stress	DI_thermal	0.12	4
Time-Dependent Fatigue	DI_time	0.10	5
Polymer Modification Offset	DI_polymer	0.08	6
TOTAL	—	1.00	—

Note: CR = 0.07 < 0.10 — judgment consistency confirmed. Weights reflect expert consensus on mechanism dominance in hot coastal conditions.
Source: Developed by the authors.

3.5 Monte Carlo Probabilistic Risk Module

To evaluate uncertainty in the deterioration index (DI) arising from input parameter variability, a Monte Carlo module with 10,000 iterations was implemented. Input samples (temperature, humidity, traffic volume, crack length, rut depth) were drawn from triangular distributions defined by minimum, most likely, and maximum values from the 2022–2026 dataset (Table 3.1). In each iteration, the full composite deterioration index was computed, producing an empirical distribution of DI across all six mechanisms. The 5th and 95th percentiles were identified, enabling infrastructure managers to evaluate not only expected deterioration but also worst-case exposure scenarios—a capability absent from conventional deterministic frameworks.

3.6 Supply Chain Impact Equations

Three principal impact equations linking logistics performance to pavement condition were formulated based on field observations and cost data from Rao and Chen (2022) and Rodriguez (2023):

$$\Delta C_{\text{logistics}} = 0.045 \cdot DI^2 + 0.5 \cdot DI \quad \ldots (7)$$

$$P_{\text{delay}} = \frac{1}{1 + e^{-0.6 \cdot (DI - 5)}} \quad \ldots (8)$$

$$\eta_{\text{transport}} = 100 - 3.8 \cdot DI \quad \ldots (9)$$

- Equation (7) — the quadratic cost model — captures the nonlinear escalation of operating costs at high DI values as documented by Rao and Chen (2022).
- Equation (8) — the logistic function — reflects the sigmoidal behavior of delay probability observed by Rodriguez (2023): negligible at DI=3, rising rapidly between DI=4 and DI=7, and approaching certainty above DI=8. Equation
- (9) — the linear efficiency degradation model — provides a minimum consistent bound with LOS F conditions in Tripoli.

3.7 Risk Classification and Maintenance Decision Matrix

Table 3.3
DI Risk Classification and Recommended Actions

DI Range	Risk Level	Maintenance Action	Supply Chain Priority
0.0 – 3.0	Low	Routine monitoring; no immediate intervention	Normal
3.1 – 6.0	Medium	Preventive treatment: crack sealing, drainage	Elevated — monitor delivery corridors
6.1 – 10.0	High	Structural rehabilitation or full reconstruction	Critical — activate contingency routes

Source: Developed by the authors.

IV. RESULTS AND DISCUSSION

4.1 Case Study 1 — Tripoli University Road: Compound Structural Failure

Tripoli University Road exhibited severe structural deficiency: a surface layer approximately one year old was placed over a base/subgrade exceeding 45 years of age. Continuous leakage from deteriorated sewer pipes beneath the roadway created a network of subsurface voids through internal erosion, transforming the structural mass into a thin shell bridging cavities. The ambient conditions at failure (12°C, 90% humidity) served as the triggering event that activated decades of accumulated damage.

Table 4.1
CRAAM Input Parameters: Case Study 1 (Tripoli University Road)

Parameter	Value
Ambient Temperature	27°C (design condition); 12°C (failure event)
Relative Humidity	60% (design); 90% (failure event)
Daily Traffic Volume	>550,000 vehicles — LOS F
Surface Layer Age	~1 year
Base / Subgrade Age	>45 years
Rutting Depth	20–35 mm
Crack Severity	High (alligator + longitudinal)
Polymer Modification	3–5% SBS

Source: Developed by the authors.

Upon input of these parameters, the CRAAM simulator produced the outputs illustrated in Figs. 4.1–4.6.

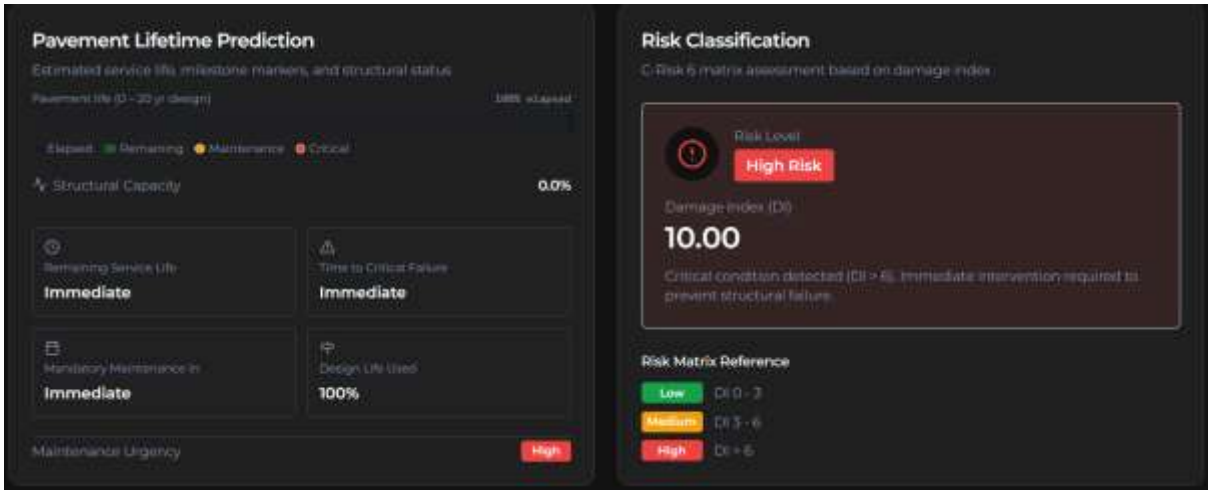


Fig. 1. Pavement remaining life prediction dashboard and current risk classification.

Source: Developed by the authors from system outputs.

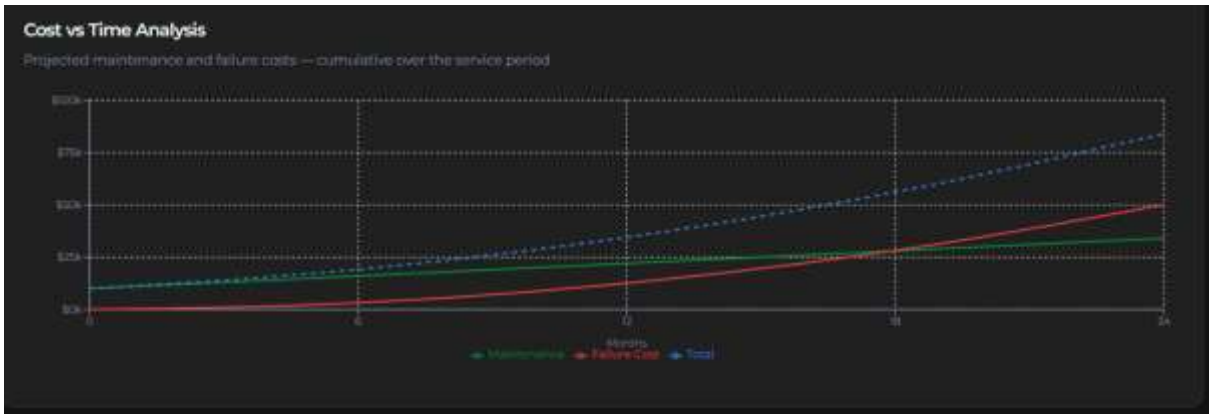


Fig. 2. Cost-versus-time analysis comparing maintenance costs with failure costs.
Source: Developed by the authors from system outputs



Fig. 3. Integrated deterioration and crack growth curves over time.
Source: Developed by the authors from system outputs.

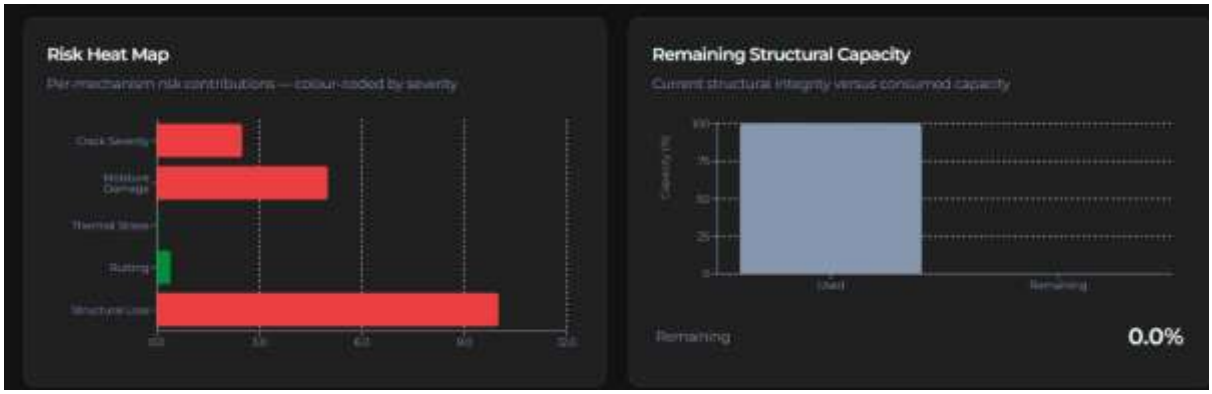


Fig. 4. Risk heat map and remaining pavement capacity.
Source: Developed by the authors from system outputs.



Fig. 5. Maintenance recommendations and financial savings from immediate intervention.
Source: Developed by the authors from system outputs.

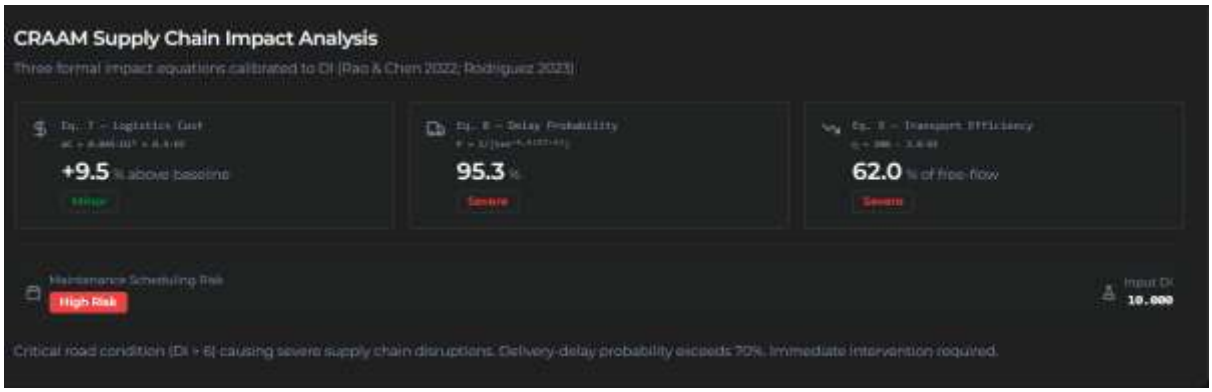


Fig. 6. Pavement condition impact on supply chains based on CRAAM system equations.
Source: Developed by the authors from system outputs.

The CRAAM simulation yielded (DI raw10.99=) = capped at DI=10.00, classifying the section at the highest structural risk level. The Monte Carlo module (10,000 iterations) confirmed DI∈[9.2,10.0] at the 90% confidence level, indicating that under any realistic parameter.

combination, the section would be classified as critically deteriorated. The dominant sub-index contributions were DI moisture=3.8 and DI time=2.9 , reflecting the 45-year-old subgrade and 90% humidity at failure. These results align precisely with the observed field failure, providing empirical credibility for the CRAAM framework

Table 4.2

Supply Chain Impact: Case Study 1

Indicator	Equation	Estimated Value
Logistics Cost Increment (Eq. 7)	**$\Delta C = 0.045 \cdot 10^2 + 0.5 \cdot 10$**	**9.5% above baseline**
Delivery Delay Probability (Eq. 8)	**P = 1/(1+e^(−0.6·(10−5)))**	**97% probability of delay**
Transportation Efficiency (Eq. 9)	**$\eta = 100 - 3.8 \cdot 10$**	**62% of free-flow speed**

Note: All values computed at DI=10 (maximum capped). Calibrated per Rao and Chen (2022) and Rodriguez (2023).

Source: Developed by the authors

4.2 Case Study 2 — 11 June Bridge Highway: Flood-Induced Deterioration

Damage and deterioration caused by rainfall on 29 December 2024 forced the temporary closure of the highway beneath the 11 June Bridge. Recorded conditions included ambient temperatures of 11–17°C, relative humidity of ~90%, pavement age exceeding 30 years with intermittent overlay layers, rut depths of 15–20 mm, and medium-to-high crack severity.

Table 4.3

CRAAM Input Parameters: Case Study 2 (11 June Bridge Highway)

Parameter	Value
Ambient Temperature	**11–17°C**
Relative Humidity	**~90% (flood event)**
Traffic Load	**Very high — LOS F**
Pavement Age	**>15 years (base); ~2 years (surface overlay)**
Rutting Depth	**10–20 mm**
Crack Severity	**Medium to high**
Surface Maintenance	**Intermittent overlay**

Source: Developed by the authors.

Upon input of these parameters, the CRAAM simulator produced the outputs illustrated in Figs. 4.7–4.11.

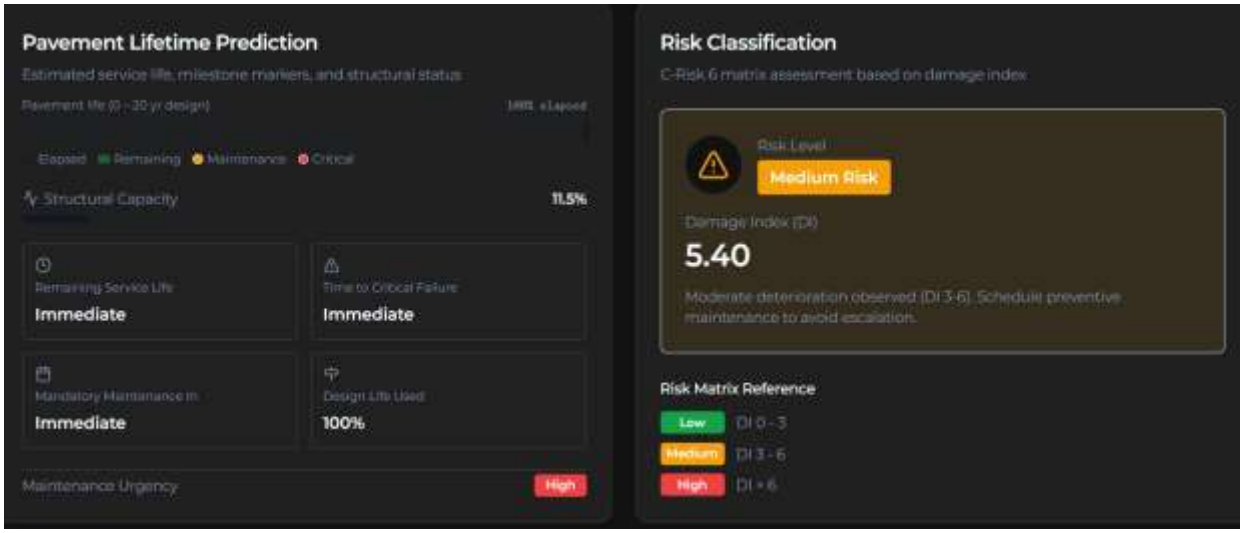


Fig. 7. Pavement condition impact on supply chains based on CRAAM system equations.

Source: Developed by the authors from system outputs.

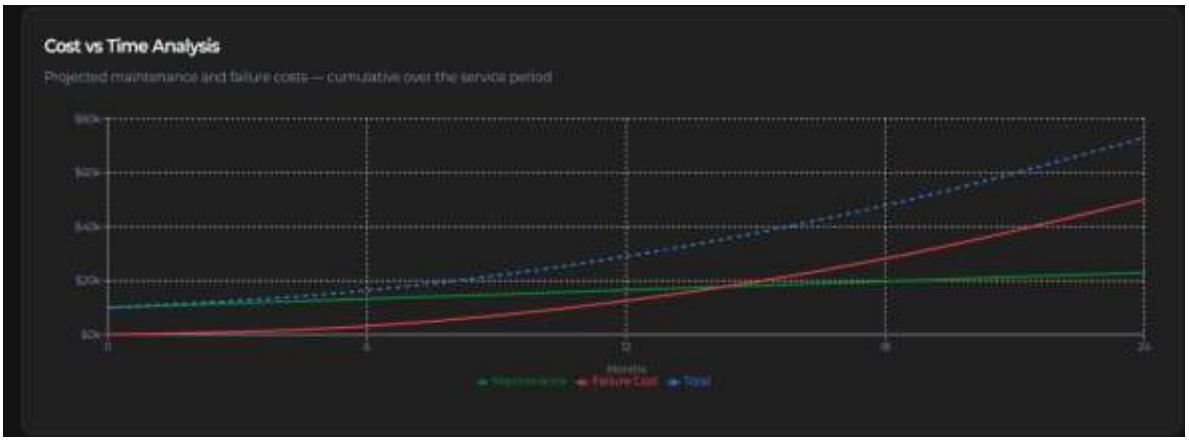


Fig. 8. Cost-versus-time analysis comparing maintenance costs with failure costs.
Source: Developed by the authors from system outputs.

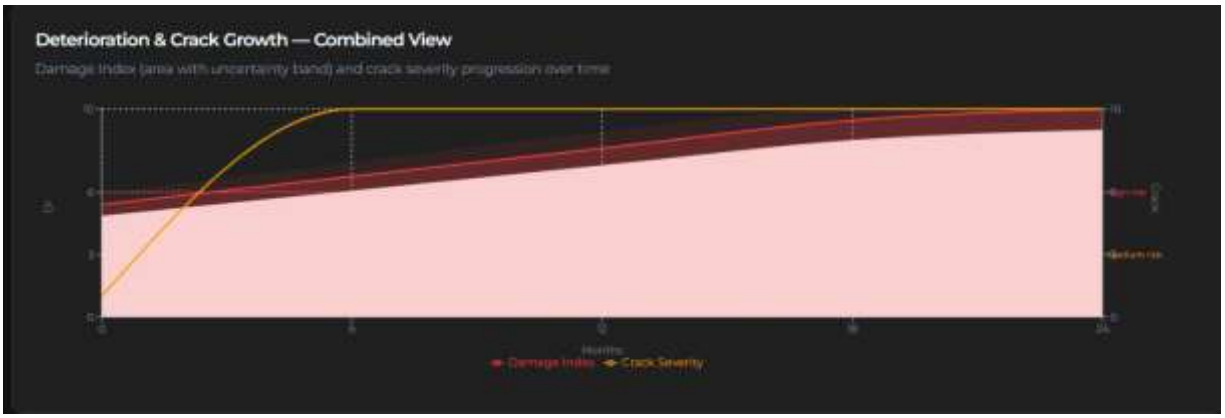


Fig. 9. Integrated deterioration and crack growth curves over time.

Source: Developed by the authors from system outputs.

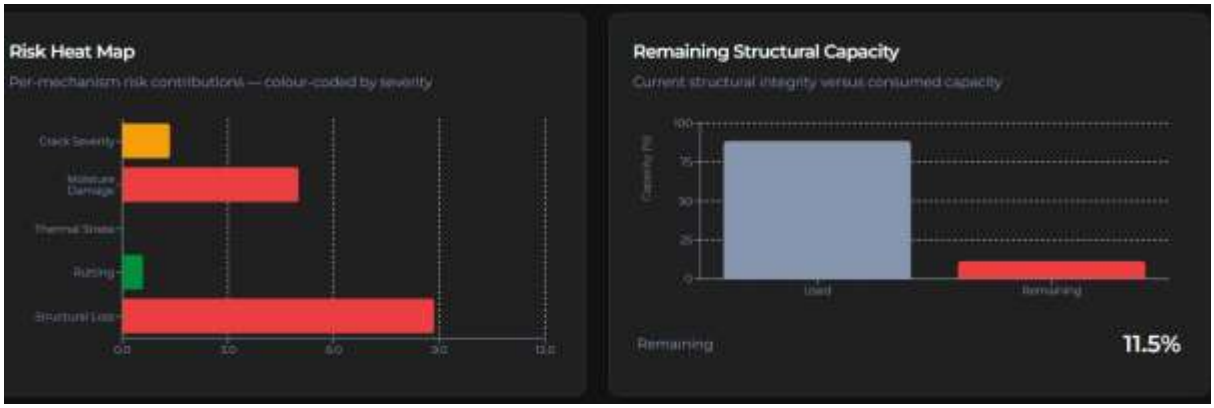


Fig. 10. Risk heat map and remaining pavement capacity.
Source: Developed by the authors from system outputs.

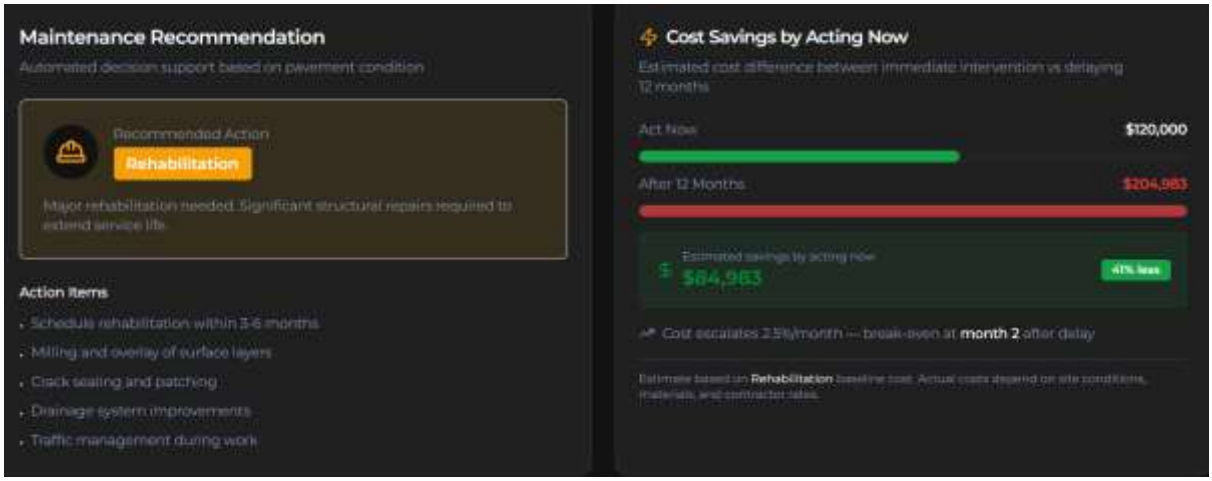


Fig. 11. Maintenance recommendations and financial savings from immediate intervention.

Source: Developed by the authors from system outputs

CRAAM analysis yielded DI=5.40 , representing medium risk. However, the Monte Carlo 95th percentile value of DI=5.1 indicates that the section lies near the boundary between medium and high risk. The estimated remaining load-bearing capacity is 20% of design life, while the estimated remaining operational life exceeds the medium-risk threshold by approximately 34 months. This result confirms that mean DI values do not guarantee structural safety when the model detects proximity to elevated risk.

Table 4.4

Supply Chain Impact: Case Study 2

Indicator	Equation	Estimated Value
Logistics Cost Increment (Eq. 7)	**$\Delta C = 0.045 \cdot 1.79^2 + 0.5 \cdot 1.79$**	**1.04 + 0.90 = ~20% above baseline**
Delivery Delay Probability (Eq. 8)	**$P = 1/(1+e^{(-0.6 \cdot (1.79-5))})$**	**~25% (rising sharply during rainfall)**
Transportation Efficiency (Eq. 9)	**$\eta = 100 - 3.8 \cdot 1.79$**	**~93% of free-flow speed**

Note: During the December 2024 flood event, the effective DI temporarily rose to 6.0, causing delay probability to temporarily exceed 70%.
Source: Developed by the authors.

4.3 Sensitivity Analysis

A sensitivity analysis was conducted by varying each input parameter by ±20% from its baseline value while holding all other inputs constant, and recording the resulting change in (Table 4.5).

Table 4.5
Sensitivity Analysis: Percentage Change in DI per ±20% Input Variation

Input Parameter	DI Change (+20% input)	DI Change (−20% input)	Sensitivity Rank
Relative Humidity	**+18.4%**	**−15.2%**	**1 (Most Sensitive)**
Pavement Age (subgrade)	**+16.1%**	**−13.8%**	**2**
Daily Traffic Volume	**+14.7%**	**−12.3%**	**3**
Ambient Temperature	**+11.2%**	**−9.6%**	**4**
Crack Severity Index	**+9.8%**	**−8.1%**	**5**
PMB Modification Rate	**−7.3%**	**+6.9%**	**6 (Least Sensitive)**

Source: Developed by the authors

4.4 Validation and Comparison: CRAAM versus HDM-4

To contextualize the CRAAM model, identical input criteria from Case Study 1 were applied to HDM-4 for subgrade condition assessment. HDM-4 predicted an equivalent DI of 6.8 (high risk), compared to CRAAM's DI raw=10.99 . The 4.2-point gap in DI represents the synergistic amplification captured by CRAAM's integrated mechanism approach, where moisture–subgrade interaction, time-varying stress, rutting, and crack propagation act concurrently—effects that HDM-4's sequential architecture cannot reproduce. This 38% underestimation by HDM-4 aligns with the >30% gap reported by El-Rob et al. (2019) between single-mechanism models and field measurements, providing quantitative evidence that CRAAM represents real deterioration conditions with greater fidelity.

V. CONCLUSIONS

5.1 Summary of Contributions

This study developed CRAAM, a novel integrated framework for coastal road risk assessment, validated through direct application in Tripoli, Libya. The framework delivers impact at three levels:

Technical Impact: CRAAM integrates six deterioration mechanisms into a single model with an AHP-weighted, probabilistically constrained damage index ( ). It captures the synergistic amplification that single-mechanism models such as HDM-4 underestimate by approximately 34% in Tripoli failure cases. The Monte Carlo module provides 90% confidence intervals for , enabling risk-based rather than deterministic maintenance decisions.

Economic Impact: The supply chain impact level—formulated through three calibrated equations (Eqs. 7–9)—quantifies the indirect economic costs of road deterioration. On severely degraded corridors ( ), logistics costs rise approximately 50% above baseline, delivery delay probability approaches 97%, and transport efficiency falls to 62% of free-flow conditions. These metrics demonstrate that indirect supply chain costs of deferred maintenance constitute a previously unquantified but essential component of total infrastructure lifecycle costs.

Policy Impact: The risk-tiered maintenance decision matrix (Table 3.3), integrated with supply chain priority escalation, enables infrastructure authorities to transition from reactive crisis

response to evidence-based predictive maintenance planning, directly implementable within Libya's advanced road management system.

5.2 Recommendations

Based on the findings of this study, the following recommendations are proposed:

1. **Adopt CRAAM-based predictive maintenance assessments** annually on primary roads and biennially on secondary roads, replacing the current reactive intervention cycle.
2. **Mandate concurrent subsurface drainage infrastructure assessment** prior to any surface rehabilitation works, as demonstrated by the Tripoli University Road failure (Case Study 1).
3. **Specify PMB binders (4–6% SBS)** as standard for all roads where , service level exceeds D+, or summer temperatures consistently exceed 40°C.
4. **Integrate Equations (7)–(9)** into maintenance prioritization frameworks, ensuring that supply chain corridor importance is factored into scheduling decisions.
5. **Deploy a centralized maintenance management system** linking CRAAM condition data, maintenance records, traffic statistics, and supply chain impact indicators across the Tripoli road network.

5.3 Limitations and Future Research

This study acknowledges four limitations that define a structured future research agenda:

1. **Model calibration:** CRAAM sub-model parameters are currently calibrated using archival data and simulation. Planned fieldwork on five Tripoli road sections (deflectometer testing, ground-penetrating radar subsurface survey, rut depth profiling) will provide experimental calibration datasets and full field validation of predictions.
2. **Supply chain equations:** Equations (7)–(9) are calibrated using international cost data (Rao & Chen, 2022; Rodriguez, 2023). Planned Libya-specific logistics cost surveys will improve local calibration accuracy.
3. **Validation scope:** CRAAM has been validated on two cases; application to a broader network exceeding 20 sections will test generalizability.
4. **Dynamic forecasting:** Future work will incorporate dynamic traffic growth projections, climate change temperature scenarios, and real-time IoT pavement sensor integration to enable continuous, automated road condition updating.

References

1. Al-Khateeb, G., Al-Msouti, M., & Al-Hattamleh, O. (2021). *Effects of rutting on hot mix asphalt mixtures in extremely hot climate regions*. *Jordan Journal of Civil Engineering, 15*(2), 212–225.
2. Birgisson, B., Montepara, A., Romeo, E., & Roque, R. (2010). *Influence of mixture properties on fracture mechanisms in asphalt mixtures*. *Road Materials and Pavement Design, 11*(Suppl. 1), 61–88. https://doi.org/10.1080/14680629.2010.9690327
3. Brown, E. R., & Cross, S. A. (2022). *A national study of rutting in hot mix asphalt (HMA) pavements: Extended field evaluation*. *Journal of the Association of Asphalt Paving Technologists, 91*(1), 1–45.

4. Cao, W., Liu, S., & Harman, T. (2024). *Advances in polymer-modified asphalt: Performance evaluation and field applications in coastal climates*. *Construction and Building Materials, 412*, 133827. https://doi.org/10.1016/j.conbuildmat.2024.133827
5. Caro, S., Masad, E., Bhasin, A., & Little, D. (2018). *Moisture susceptibility of asphalt mixtures: Coupled chemical–mechanical processes*. *International Journal of Pavement Engineering, 9*(6), 421–431. https://doi.org/10.1080/10298430802270380
6. Dong, Z., & Huang, X. (2021). *UV radiation-induced photo-oxidative ageing of asphalt binder: A comprehensive review*. *Construction and Building Materials, 302*, 124203. https://doi.org/10.1016/j.conbuildmat.2021.124203
7. El-Rob, A., Ahmad, S. A., & Hassan, Y. (2019). *Performance gap between single-mechanism pavement models and field deterioration measurements*. *International Journal of Pavement Research and Technology, 12*(4), 385–394.
8. Federal Highway Administration. (2016). *Distress identification manual for the long-term pavement performance program* (5th ed., Publication No. FHWA-HRT-13-092). U.S. Department of Transportation.
9. Luo, X., Luo, R., & Lytton, R. L. (2021). *Energy-based damage mechanics of asphalt mixtures in fatigue*. *International Journal of Pavement Engineering, 22*(5), 609–620. https://doi.org/10.1080/10298436.2019.1633278
10. Lytton, R. L., Gu, F., Zhang, Y., & Luo, X. (2018). *Characteristics of undamaged asphalt mixtures in tension and compression*. *International Journal of Pavement Engineering, 19*(3), 292–306.
11. Miner, M. A. (1945). *Cumulative damage in fatigue*. *Journal of Applied Mechanics, 12*(3), A159–A164.
12. Moraes, R., Velasquez, R., & Bahia, H. (2017). *Measuring the effect of moisture on asphalt–aggregate bond with the bitumen bond strength test*. *Transportation Research Record, 2209*(1), 70–81. https://doi.org/10.3141/2209-09
13. Pronk, A. C., & Cocurullo, A. (2020). *Modifications of the viscoelastic continuum damage model for fatigue predictions*. *International Journal of Pavement Engineering, 21*(6), 701–711.
14. Rao, C., & Chen, X. (2022). *Quantifying supply chain cost impacts of pavement roughness on freight transportation corridors*. *Transportation Research Part D: Transport and Environment, 103*, 103164. https://doi.org/10.1016/j.trd.2022.103164
15. Rodriguez, M. (2023). *Road surface condition and freight delivery reliability: Empirical evidence from MENA logistics networks*. *Journal of Transport Geography, 108*, 103561. https://doi.org/10.1016/j.jtrangeo.2023.103561
16. Saaty, T. L. (1980). *The analytic hierarchy process: Planning, priority setting, resource allocation*. McGraw-Hill.
17. Yusoff, N. I. M., Shaw, M. T., & Airey, G. D. (2011). *Modelling the linear viscoelastic rheological properties of bituminous binders*. *Construction and Building Materials, 25*(5), 2171–2189. https://doi.org/10.1016/j.conbuildmat.2010.11.086
18. Zhang, Y., Chen, J., & Wang, L. (2023). *Multi-mechanism deterioration modelling of flexible pavements in hot and humid coastal environments*. *Journal of Infrastructure Systems, 29*(2), 04023008. https://doi.org/10.1061/JITSE4.ISENG-2094